Accepted Manuscript

Synthesis and Characterisation of Novel Yellow Azo Dyes from 2-Morpholin-4-yl-1,3-thiazol-4(5H)-one and Study of Their Azo-Hydrazone Tautomerism

Prashant G. Umape, Vikas S. Patil, Vikas S. Padalkar, Kiran R. Phatangare, Vinod D. Gupta, Abhinav B. Thate, Nagaiyan Sekar

Please cite this article as: Umape PG, Patil VS, Padalkar VS, Phatangare KR, Gupta VD, Thate AB, Sekar N, Synthesis and Characterisation of Novel Yellow Azo Dyes from 2-Morpholin-4-yl-1,3-thiazol-4(5H)-one and Study of Their Azo-Hydrazone Tautomerism, *Dyes and Pigments* (2013), doi: 10.1016/j.dyepig.2013.05.002.

Synthesis and Characterisation of Novel Yellow Azo Dyes from 2-Morpholin-4-yl-1,3-thiazol-4(5*H*)-one and Study of Their Azo-Hydrazone Tautomerism.

Prashant G. Umape, Vikas S. Patil, Vikas S. Padalkar, Kiran R. Phatangare,

Vinod D. Gupta, Abhinav B. Thate, Nagaiyan Sekar*

Tinctorial Chemistry Group, Department of Dyestuff Technology,

Institute of Chemical Technology, Nathalal Parekh Marg, Matunga, Mumbai - 400 019. (India)

*Corresponding author. Tel.: +91 22 3361 1111/2222, 2707(direct), Fax.: +91 22 3361 1020.

E-mail: n.sekar@ictmumbai.edu.in, nethi.sekar@gmail.com

Abstract:

Novel yellow azo dyes were synthesized by diazotization of aromatic amines followed by coupling with 2-morpholin-4-yl-1,3-thiazol-4(5*H*)-one and fully characterized. The geometries of the synthesized dyes for azo and hydrazone tautomeric forms were optimized using B3LYP, CAM-B3LYP and M06 functional and 6-31G(d) and 6-311++G (d,p) basis sets, also their electronic excitation properties were evaluated using density functional theory. The optimized geometries reveal that the hydrazone for is more stable than the azo form. Photophysical properties of the synthesized dyes were evaluated by UV-Visible spectroscopy and compared with computed vertical excitation obtained from TDDFT. The results clearly illustrate existence of dye **8a**, **8b** and **8c** in hydrazone tautomeric form, while **8d** exist in both azo as well as hydrazone form. Thermal stabilities were estimated by using thermo gravimetric analysis, and results revels that the synthesized dyes have good thermal stability.

Keywords: Yellow azo dyes, 2-(Morpholin-4-yl)-1,3-thiazol-4(5*H*)-one, Diazotization, Diazocoupling, Density functional theory, Azo-hydrazone tautomerism.

1. Introduction

Azo chromophores have versatile applicability ranging from textile dyeing [1], leather dyeing [2], coloring of plastics and polymer [3] to advanced applications such as liquid crystal displays [4], biological and medical studies and advanced application in organic synthesis [5]. Also, they contribute greatest production volume of the dyestuff industry due to simplistic mode of their synthesis with high yield.

Azo colorants derived from aromatic heterocyclic amines or coupling components have excellent light and sublimation fastness, color strength and bright hue [6]. Thiazole based azo colorants have been reported as disperse dyes for polyester, with excellent wash fastness and good sublimation fastness [7]. They find use in spectrophotometric determination of Iron (III) [8]. A few thiazole containing azo dyes have been reported as antimicrobial agents [9-12].

The existence of azo-hydrazone equilibrium in azo colorants having hydroxy group at *ortho* or *para* to azo linkage was first proved by Kuhn and Bar, which was postulated by Liebermann in 1983 [13]. Due to the hydrogen bonding in hydrazone tautomeric form it forms a linear and coplanar six membered ring having higher thermal stability than those with the azo forms [14]. This tautomerism of azo benzene derivatives leads to their applicability as biomarkers [15], chemical sensors [16]. Also the azo chromophoric system gives carcinogenic amines after reductive cleavage [17], while the hydrazone tautomer will cleave the C-N bond instead of N=N bond [18]. Hence, the study of azo-hydrazone tautomerism will give significant information for

proposing efficient process for degradation of azo chromophores with least toxicological effect on environment.

In this paper, we report synthesis of novel azo chromophores by diazotization of aromatic amines followed by coupling with 2-morpholin-4-yl-1,3-thiazol-4(5H)-one [19]. The absorption spectra were measured using UV-Visible spectrophotomerer and thermal stabilities were determined by using thermogravimetric analysis (TGA). The structures of the synthesized dyes were confirmed by spectral analysis. Density functional theory was used to study their azo-hydrazone tautomerism. The structures of dyes in azo and hydrazone forms were optimized in the ground state using B3LYP, CAM-B3LYP and M06 functional and 6-31G(d) and B3LYP/6-311++ G(d,p) basis sets. Synthesized compounds are summarized (**Figure 1).**

Insert Figure 1.

Insert Scheme 1.

2. Experimental

2.1. Materials and equipments

Ammonium thiocyanate, benzoyl chloride, morpholine, ethyl chloroacetate were procured from s. d. fine chemicals (India) and used without further purification. All other chemicals used were of laboratory grade and used without purification. The reaction was monitored by TLC using on 0.25 mm E-Merck silica gel 60 F_{254} precoated plates, which were visualized under UV light. Melting points were measured by open capillary method on standard melting point apparatus from Sunder industrial product Mumbai, and are uncorrected. The FT-IR

3

spectra were recorded on a Perkin-Elmer Spectrum 100 FT-IR Spectrometer using KBr discs. ^{1}H NMR spectra were recorded on VXR 300 MHz instrument using TMS as an internal standard. The UV Visible absorption spectra of the dyes were recorded on a Spectronic Genesys 2 UV-Visible spectrophotometer. TGA measurements were performed out on SDT Q600 v8.2 Build 100 model of TA instruments Waters (India) Pvt. Ltd.

2.2. Synthesis and characterization

2.2.1. Preparation of silica gel-supported ammonium thiocyanate

Silica gel (40 g) was added to a solution of ammonium thiocyanate (5 g, 65.7 mmol) in dry acetonitrile (125 mL), and the mixture was stirred at room temperature for 30 min. Acetonitrile was removed under reduced pressure at 50 $^{\circ}$C. The resulting silica gel-supported ammonium thiocyanate was dried in vacuo (10 mmHg) at room temperature for 3-4 h [20a].

2.2.2. Synthesis of N-[(morpholin-4-yl)carbonothioyl]benzamide(3)

To a slurry of NH_4SCN/SiO_2 (45 g, 65.7 mmol) in 1,2-dichloroethane (150mL), benzoyl chloride (3.81 mL, 32.8 mmol) was added slowly for 30 min and stirred at 25-30 $^{\circ}$C for 2 h. Then morpholine (5.72 mL, 65.7 mmol) was added to it and stirred for an additional 2 h. The reaction mixture was filtered to remove the supported reagent, residual silica was again washed by 1,2-dichloroethane and filtered. The combined filtrate was washed with 5% HCl and then with brine solution, and dried over Na_2SO_4. The solvent was evaporated under reduced pressure to leave the crude product **3**, which was purified by column chromatography silica gel 100-200 mesh and toluene as eluent system. [20a]

Yield: 65%, Melting point: 153-156 °C (155-157 °C lit[20b])

2.2.3. Synthesis of morpholine-4-carbothioamide (*4*)

 N-(Morpholin-4-yl-carbonothioyl) benzamide (**3**) (10.50 g 41.9 mmol)was charged in conc. HCl (20 mL) and the mixture is stirred at 75-80 $^{\circ}$C for 4 h, completion of the reaction was monitored by TLC. The reaction mixture then brought to room temperature then neutralized with liq. ammonia, extracted with 1,2-dichloroethane dried over Na_2SO_4 and solvent removed under reduced pressure. The resulting crude mass was recrystallized from ethanol as a solvent [20b].

Yield: 78%, Melting point: 176-177 °C (177-178 °C lit[20b])

2.2.4. Synthesis of 2-(morpholin-4-yl)-1,3-thiazol-4(5H)-one hydrochloride (*5*)

Morpholine-4-carbothioamide(4) (5 g, 34.2 mmol) and ethyl chloroacetate (4 mL, 37.6 mmol) were heated to reflux for 3 h in ethanol, completion of the reaction was monitored by TLC. Diethyl ether was added to the resulting reaction mass slowly and precipitated product filtered off dried [19].

Yield: 61%, Melting point: 178-180 °C (174-178 °C lit[19])

2.2.5. Preparation of azo dyes (**8a-8e**)

2.2.5.1. General procedure for diazotization of aniline derivatives

Aniline derivative, (22.4 mmol) was dissolved in 5N HCl (30 mL) and the solution was then cooled to 0-5 $^{\circ}$C. Sodium nitrite (1.7 g, 24.7 mmol) dissolved in H_2O (3 mL) was added to the above solution drop wise maintaining the temperature 0-5 °C and stirred for 1 h. The resulting diazonium solution (**7a-7e**) was further used immediately for coupling.

2.2.5.2. General procedure for coupling

The coupling component, 2-(morpholin-4-yl)-1,3-thiazol-4(5*H*)-one hydrochloride (**5**) (5 g 22.4 mmol) were dissolved in acetic acid and then cooled to 0-5 $^{\circ}$C. The diazonium solution

previously prepared was added drop wise maintaining the temperature 0-5 °C, pH 4-5 maintained by using sodium acetate. The reaction mixture further stirred for 30-35 h for completion for coupling. Precipitated product filter and washed with water, crystallized from DMF. Yields, physical properties and characterization data are summarized in (**Tables 1-2**).

3. Results and discussion

3.1. Synthesis of dyes

A simple and facile synthetic route was adapted for the synthesis of azo dyes. The key intermediate 2-(morpholin-4-yl)-1,3-thiazol-4(5*H*)-one **5** was synthesized from morpholine-4-carbothioamide **4** by refluxing with ethyl chloroacetate in ethanol as a solvent. Morpholine-4-carbothioamide **4** was obtained from ammonium thiocyanate and benzyl chloride **Scheme 1**. Benzoyl isothiocyanate **2** was formed by the reaction of benzoyl chloride **1** with silica gel supported ammonium thiocyanate (NH$_4$SCN/SiO$_2$). Further benzoyl isothiocyanate on reaction with morpholine yield *N*-[(morpholin-4-yl)carbonothioyl]benzamide **3** [20a]. The debenzoylation of *N*-[(morpholin-4-yl)carbonothioyl]benzamide **3** gives morpholine-4-carbothioamide **4** in good yield [20b].

Morpholine-4-carbothioamide **4** with ethyl chloroacetate in refluxing ethanol gives a key intermediate 2-(morpholin-4-yl)-1,3-thiazol-4(5*H*)-one **5 [19]**. Different aniline derivatives **6** have been diazotized by using NaNO$_2$ in HCl-water mixture (1:1) and further coupled with the synthesized coupling component 2-(morpholin-4-yl)-1,3-thiazol-4(5*H*)-one **5** to obtain the respective azo dyes **8a-8e** in good yields (**Table 1**). Infrared spectra (**Table 2**) of the synthesized chromophore **8a** show carbonyl band at 1666 cm^{-1} and absence of broad band for hydroxyl group gives indication that the chromophore may exist in tautomeric form of azo-hydrazone. ^{1}H NMR

6

spectra summarised in (**Table 2)** indicates the dye **8a** shows a singlet at δ 10.5 ppm attributed to N-H proton which is in hydrazone form. The characteristic doublet for aromatic proton appears at δ 7.36 and 7.24 ppm, triplet at δ 3.9 and 3.6 ppm and multiplate at δ 3.7 ppm was attributed to morpholine protons.

Insert Table 1.

Insert Table 2.

3.2. Photo-physical properties

To find out structural correlation with colour properties of synthesized azo dyes, UV-Visible spectra of the dyes were recorded in DMF and the results are tabulated in (**Table 3**). The absorption spectra of these dyes showed absorption band in the region 368-535 nm, with shoulder peaks ranging from 268-304 nm. The bathochromic shift was observed in the absorption spectra, when halo substituent altered from chlorine **8a** (371 nm) to fluorine **8b** (406 nm), while *m*-nitro derivative **8d** has red shifted absorption (425 nm) than *p*-nitro derivative **8c** (368 nm). The 2,4-dinitro substituted azo chromophore **8e** absorbs at 535 nm. These strong absorption bands are attributed to the π—π* transitions involving the charge transfer (CT) throughout the whole molecular π-electronic system. Dyes **8a** and **8c** has shoulder peak at 299 nm, while dyes **8b, 8d** and **8e** showed absorption spectra with shoulder peaks at 304, 281 and 268 nm respectively. The shoulder peak observed may be due to the π—π* transitions within the aromatic fragment with molar extinction coefficient in the range 8636-13278. The Absorption

7

spectrum of dye **8d** has one more peak at 344 nm, which indicate the existence of both azo as well as hydrazone form in DMF. The peak at 344 nm can be attributed to azo form, as hydrazone form absorbs at higher wavelength than azo form with high colour strength [21].

Insert Table 3

3.3. Computational study

Gaussian 09 program package was employed to optimize geometry and to study profusion of the synthesized azo dyes in their azo and hydrazone tautomeric forms. [22]. Ground state (S_0) geometry of the reported dyes in gas phase and DMF was optimized in their C_1 symmetry using DFT [23]. The Becke's three parameter exchange functional (B3) [24] combining with nonlocal correlation functional by Lee, Yang and Parr (LYP) [25], long range corrected CAM-B3LYP and highly parameterized empirical M06 were used; the computations were performed using basis sets 6-31G(d) and 6-311++G(d,p) for all atoms. Further the local minima on the energy surface of the optimized structure were verified by computing the vibrational frequencies using the same methods. Time Dependent Density Functional Theory (TDDFT) using the same hybrid functional and basis sets was carried out to obtain vertical excitation energies and oscillator strengths at the optimized ground state equilibrium geometries [26]. On the basis of the optimized ground structures absorption characteristics, oscillator strengths and configuration were systematically evaluated using TDDFT with polarizable continuum model PCM model.

8

3.3.1. Optimized geometries of azo-hydrazone tautomeric forms

The optimized ground state geometries of the dyes in their azo-hydrazone tautomeric forms are summarized in (**Table 4**). Optimized ground state geometries of these azo dyes are planar except the azo chromophore **8e** with dinitro substitution on aniline ring. The dye **8e** has dihedral angular twist by 24.57º at N20-N21-C22-C27 with B3LYP/6-31G(d) and dihedral angular twist by 23.22º at N20-N21-C22-C27 with B3LYP/6-311++G(d,p) level (**Figure 2**). While hydrazone form of the dye **8e** has twisted dihedral angle of 19.87 º and 18.55º at N20-N21-C22-C27 with B3LYP/6-31G(d) and B3LYP/6-311++G(d,p) levels respectively (**Figure 3**). The dihedral angular twist for the azo dye **8e** using CAM-B3LYP and M06 functional are 28.47º at 6-31G(d), 26.62º at 6-311++G(d,p) basis set and 25.77º at 6-31G(d), 23.68º at 6-311++G(d,p) basis set respectively. Also the dihedral angular twist for hydrazone form of azo dye **8e** using CAM-B3LYP and M06 functional are as follows 22.14º at 6-31G(d), 20.29º at 6-311++G(d,p) basis set and 20.45º at 6-31G(d), 18.35º at 6-311++G(d,p) basis set.

Optimized bond lengths of the synthesized dyes **8a-e** are tabulated (**Table 5, Supporting information Table 2-15).** The O-H bond lengths of azo forms for the series are 1.011, 1.010, 1.015, 1.012, 1.013 Å at B3LYP/6-31G(d) and 1.006, 1.005, 1.011, 1.007, 1.008 Å at B3LYP/6-311++G(d,p) levels for dyes **8a-8e**. While the O-H bond lengths for azo forms optimized using CAM-B3LYP functional are found to be 1.005, 1.004, 1.010, 1.007, 1.009 at 6-31G(d) and 1.001, 1.000, 1.007, 1.003, 1.006 at 6-311++G(d,p) levels. Also using M06 functional the optimized O-H bond lengths are 1.002, 1.001, 1.005, 1.003, 1.004 at 6-31G(d) level and 0.997, 0.996, 1.000, 0.998, 0.998 at 6-311++G(d,p) level. The increased O-H bond length is due to the hydrogen bonding between N21 and H atom. While the hydrogen bonding between N21···H34,

9

N21⋯H34, N21⋯H36, N21⋯H36 and N21⋯H38 for **8a-8e** chromophores are 1.732, 1.740, 1.711, 1.723, 1.716 at B3LYP/6-31G(d) and 1.729, 1.736, 1.700, 1.717, 1.712 at B3LYP/6-311++G(d,p) levels of calculations. Similarly with CAM-B3LYP/6-31G(d) level the N⋯H bond lengths are 1.734, 1.743, 1.709, 1.723, 1.706 and at CAM-B3LYP/6-311++G(d,p) level the optimized N⋯H bond lengths are 1.729, 1.738, 1.696, 1.714, 1.695. While the optimized N⋯H bond lengths for the azo chromophores using M06 functional are 1.775, 1.777, 1.758, 1.767, 1.759 at 6-31G(d) level and 1.773, 1.775, 1.749, 1.759, 1.754 at 6-311++G(d,p) level.

Hydrazone form of the featuring chromophores have optimized geometry with interatomic distance for O33⋯H34, O33⋯H34, O35⋯H36, O35⋯H36, O37⋯H38 at B3LYP/6-31G(d) and B3LYP/6-311++G(d,p) levels of calculations are 1.904, 1.907, 1.897, 1.896, 1.873 Å and 1.923, 1.924, 1.912, 1.913, 1.888 Å. As well as at CAM-B3LYP/6-31G(d) and CAM-B3LYP/6-311++G(d,p) levels the optimized O⋯H bond lengths for hydrazone from are 1.895, 1.897, 1.888, 1.888, 1.868 and 1.913, 1.913, 1.903, 1.904, 1.882 respectively. Similarly using M06 functional the optimized O⋯H bond lengths are as follows 1.907, 1.909, 1.902, 1.922, 1.888 at B3LYP/6-31G(d) level and 1.916, 1.919, 1.907, 1.928, 1.896 B3LYP/6-311++G(d,p) level. The N-H bond lengths between N21-H34, N21-H34, N21-H36, N21-H36 and N21-H38 for the series **8a-8e** at both the levels of calculations are as follows 1.024, 1.024, 1.025, 1.024, 1.026 Å and 1.023, 1.024, 1.023, 1.023, 1.025 Å. Subsequently the optimized N-H bond lengths for hydrazone form using CAM-B3LYP functional at both the levels of computations are 1.022, 1.022, 1.022, 1.022, 1.023 and 1.020, 1.020, 1.021, 1.021, 1.022 respectively. While using M06 functional the respective N-H bond lengths are 1.026, 1.026, 1.026, 1.025, 1.027 at 6-31G(d) level and 1.025, 1.024, 1.025, 1.024, 1.026 at 6-311++G(d,p) level. The N-H bond lengths

observed are slightly longer than the actual N-H bond length of 1.01 Å which is due to O···H hydrogen bonding.

The N20-N21 bond lengths for azo forms are 1.294, 1.292, 1.301, 1.297, 1.307 Å and 1.289, 1.287, 1.297, 1.292, 1.303 Å at B3LYP/6-31G(d) and B3LYP/6-311++G(d,p) levels of calculations. While using CAM-B3LYP/6-31G(d) and CAM-B3LYP/6-311++G(d,p) levels of calculations the N-N bond lengths in azo forms are 1.278, 1.276, 1.285, 1.281, 1.293 and 1.272, 1.270, 1.280, 1.276, 1.290 Å respectively. At M06/6-31G(d) and M06/6-311++G(d,p) levels of calculations the N-N bond lengths in azo forms are of 1.285, 1.283, 1.292, 1.288, 1.299 and 1.279, 1.277, 1.287, 1.282, 1.295 Å. These optimized N-N bond lengths are longer than the usual value 1.24 Å. While in hydrazone form N20-N21 bond lengths are 1.329, 1.327, 1.386, 1.333, 1.342 and 1.327, 1.325, 1.386, 1.331, 1.341 at B3LYP /6-31G(d) and B3LYP/6-311++G(d,p) levels of calculations. Similarly the N-N bond lengths at CAM-B3LYP functional in hydrazone form are 1.323, 1.321, .330, 1.327, 1.338 at 6-31G(d) level and 1.321, 1.320, 1.329, 1.326, 1.337 at 6-311++G(d,p) level . Also at M06/6-31G(d) and M06/6-311++G(d,p) levels of calculations the N-N bond lengths in hydrazone forms are 1.323, 1.320, 1.330, 1.327, 1.337 and 1.319, 1.318, 1.327, 1.324, 1.335. These obtained N-N bond lengths in hydrazone form falls shorter to the model value of 1.40 Å for single bond [27]. The N20-N21 bond length values obtained for azo and hydrazone form signify the single-double bond character of the bond and confirms the azo-hydrazone tautomerism in the synthesized molecules.

Insert Figure 2.

Insert Figure 3.

Insert Table 5.

3.3.2. Calculated energies of azo-hydrazone tautomeric forms

Calculated energies (E/hartree), Gibbs free energies (ΔG/hartree) and relative energies (ΔE/kJ mol^{-1}) of the chromophores **8a-8e** in their azo and hydrazone tautomeric forms at both the levels of calculation so as to check the more stable form and the values are tabulated in (**Table 6-7, supporting info. Table 16-19**). From the **Table 6** it is clear that the hydrazone form is relatively more stable than the corresponding azo form by 50.40, 49.06, 53.27, 50.54, 46.77 and 44.98, 43.80, 47.86, 45.02, 40.80 kJ mol $^{-1}$ at B3LYP /6-31G(d) and B3LYP/6-311++G(d,p) levels in gas phase. The Calculated energies (E/(ΔG/hartree) and relative energies (ΔE/kJ mol^{-1}) in DMF as a solvent also shows that the hydrazone form is having more stability than azo form by 50.40, 49.00, 53.89, 50.66, 47.70, and 44.79, 43.49, 48.62, 45.01, 42.02 kJ mol $^{-1}$ at B3LYP /6-31G(d) and B3LYP/6-311++G(d,p) levels of calculation respectively **(Table 7)**. At CAM-B3LYP /6-31G(d) the hydrazone form have stability by 50.73, 50.80, 56.43, 53.06, 50.42 kJ/mol^{-1} and at CAM- B3LYP/6-311++G(d,p) levels of calculations hydrazone form is more stable than azo form by 47.30, 45.64, 51.18, 47.73, 44.90 kJ/mol^{-1} in gas phase (Supporting info. Table 16). Similarly in DMF hydrazone form have more stability than azo form by 59.58, 57.97, 63.03, 59.65, 56.11 kJ/mol^{-1} at CAM-B3LYP /6-31G(d) and 56.70, 55.22, 59.90, 56.42, 52.28 kJ/mol^{-1} at CAM- B3LYP/6-311++G(d,p) level (Supporting info. Table 17). The energy data obtained by calculation carried our using M06 functional shows that the hydrazone form of the dyes are

12

energetically more stable then the azo form by 50.83, 50.24, 55.13, 52.09, 47.80 kJ/mol[-1] at M06/6-31G(d) level and 44.79, 43.49, 48.63, 45.02, 42.02 kJ/mol[-1] at M06/6-311++G(d,p) level of calculation in gas phase (SI **Table 18**). Similar trend is observed in DMF using M06/6-31G(d) and M06/6-311++G(d,p) levels of calculations and the stability of hydrazone form over the azo form is by 58.45, 56.99, 60.73, 58.30, 52.15 and 54.97, 53.81, 57.31, 54.76, 48.44 kJ/mol[-1] respectively(SI **Table 19**).

Insert Table 6.

Insert Table 7.

3.3.3. Electronic vertical excitation spectra

The calculated excitation spectra using B3LYP, CAM-B3LYP and M06 functional at 6-31G(d) and 6-311++G(d,p) levels in gas phase as well as in DMF, their oscillator strength (*f*), orbital contribution and band gap are shown in (Supporting info. **Tables 20-31**) with their experimental excitation spectra. The chromophore **8a** has absorption at 371 nm in DMF, its calculated vertical excitation at 6-31G(d,) level is 434, 400, 428 nm for azo tautomer and 390, 342, 378 nm for hydrazon tautomer in DMF using B3LYP, CAM-B3LYP and M06 functional respectively, while at B3LYP/6-311++G(d,p) level 445, 409, 438 nm for azo and 404, 351, 387 nm for hydrazone tautomer. In gas phase vertical excitation is 410, 378, 404 nm and 380, 333, 368 nm at 6-31G(d) level of calculation; for 6-311++G(d,p) level 418, 84, 412 nm and 387, 340, 376nm excitation was resulted for azo and hydrazone tautomers respectively. The experimental λ_{max} and computed vertical excitation values at both the levels of calculation for azo as well as hydrazone tautomeric

13

form gives conformation of the existence of compound **8a** in hydrazone form in gas phase and in DMF. Shoulder peak at 299 nm attributed to HOMO-1 to LUMO transition, also vertical excitation spectra of optimized hydrazone form in DMF have shoulder peak at 288, 253, 266 nm for 6-31G(d) and 293, 257, 269 nm for 6-311++G(d,p) levels of calculations. Such shoulder peak is not observed in optimized azo form. The computed vertical excitation values for chromophore **8b** at 6-31G(d) is 429,395, 422 nm for azo form and 391, 344, 379 nm for hydrazone form, also 439, 404, 431 nm for azo and 397, 350, 384 for hydrazone form vertical excitation is observed at 6-311++G(d,p) level. Experimental absorbance is found to be 406 nm with shoulder peak at 304 nm. The shoulder peak observed at 286, 251, 263 nm and 290, 256, 266 nm only for hydrazone form at both the levels of optimisation resembles the 304 nm experimental value suggest existing hydrazone form for dye **8b**. While in gas phase 404, 373, 398 nm and 411, 380, 405 nm for azo form are the closest values with the actual values, but shoulder peak was not observed for both azo as well as hydrazone form. Dye **8c** also concludes their existence in hydrazone tautomeric form. The shoulder peak observed at 299 nm has not seen in computed excitation pattern in DMF at both the levels of calculation using B3LYP functional, while it has been observed in DMF using M06 functional at 291 and 297 nm for hydrazone form. The shoulder peak observed in gas phase computation at 293, 263, 278 nm and 297, 254, 282 nm corresponding to HOMO-1→LUMO excitation. Dye **8d** shows absorption with 281 nm shoulder peak and other two peaks at 344 nm and 425 nm. Computed vertical excitation pattern for dye **8d** shows shoulder peak at 291, 254, 277 nm and 294, 258, 280 nm in DMF at 6-31G(d) and 6-311++G(d,p) levels of calculations, while 283, 249, 271nm in gas phase at 6-31G(d) level. Vertical excitation of the dye optimized at 6-31G(d) and 6-311++G(d,p) levels using B3LYP, CAM-B3LYP and M06

functional are 428, 397, 421 and 438, 407, 431 nm in DMF, while 402, 374, 396 and 456, 381, 401 nm in gas phase for azo form corresponding to the experimentally observed peak at 425 nm. The hydrazone form has 375, 334, 363and 383, 340, 371 nm in DMF. While vertical excitation observed in gas phase are 363, 324, 351 and 368, 329, 357 nm respectively corresponding to the actual peak observed at 344 nm. All these values obtained by experimental and computation method indicates existence of both azo and hydrazone forms for dye **8d**. Dye **8e** has absorbance at 535 nm and shoulder peak is observed at 268 nm, In DMF computed vertical excitation values for optimized azo form show resemblance with the experimental values for B3LYP and M06 functional i.e. at 498, 479 and 517, 492 nm but in gas phase a large difference is observed in actual and computed values.

3.4. Thermal stability of dyes

Thermal stabilities of the synthesized azo dyes were investigated by thermogravimetric analysis (TGA). The TGA data obtained are summarized in (**Table 1**). The overlay TGA analysis curves for the azo dye **8a-8e** under nitrogen atmosphere (**Figure 4**) showed no weight loss up to 100-150 °C, indicating absence of water molecules and/or any other adsorptive solvent molecules. The TGA curves shown in the (**Figure 4**) indicate that these dyes are having good thermal stability and a steep weight loss observed from 255 °C. Dye **8b** with *p*-fluoro substituent in phenyl ring is having good thermal stability (316 °C) amongst other synthesized dyes.

Insert Figure 4

15

4. Conclusions

In summary, we have developed an efficient and simple protocol for the synthesis of novel azo dyes from 2-morpholin-4-yl-1,3-thiazol-4(5*H*)-one. Synthesized dyes were confirmed by FT-IR, ^{1}H NMR and mass spectral analysis. The TGA results show that they are having good thermal stability. The optimized structure of azo as well as hydrazone form at B3LYP/6-31G(d) and B3LYP/6-311++G(d,p) levels of calculations and their calculated energies (E/(ΔG/hartree), relative energies (ΔE/kJ mol^{-1}) shows that the hydrazone form is having more stability than azo form. The experimental and computed vertical excitation spectrum clearly indicates existence of dye **8a**, **8b** and **8c** in hydrazone tautomeric form, while **8d** exist in both azo as well as hydrazone form.

Acknowledgements

References

[1] Koh J, Greaves AJ. Synthesis and application of an alkali-clearable azo disperse dye containing a fluorosulfonyl group and analysis of its alkali-hydrolysiskinetics, Dyes and Pigments 2001;50:117-126.

[2] Vijayaraghavan R, Vedaraman N, Surianarayanan M, MacFarlane DR. Extraction and recovery of azo dyes into an ionic liquid. Talanta 2006;69(5):1059-1062.

[3] Machida S, Araki M, Matsuo K. Studies of the water-soluble polymers. XVI. Azo dyes of poly-*N*-vinylimidazole. J App Poly Sci 1968;12(2):325–332.

[4] George WG. Dyes and liquid crystals. Dyes and Pigments 1982;3:203-209.

[5] Nejati K, Rezvani Z, Seyedahmadian M. The synthesis, characterization, thermal and optical properties of copper, nickel, and vanadyl complexes derived from azo dyes. Dyes and Pigments 2009;83:304–311.

[6] Hu B, Wang G, You W, Huang W, You X. Azo-hydrazone tautomerism by *in situ* Cu^{II} ion catalysis and complexation with the H_2O_2 oxidant of C.I. Disperse Yellow 79. Dyes and Pigments 2011;91:105-111.

[7] Metwally MA, Abdel-latif E, Amer FA, Kaupp G. Synthesis of new 5-thiazolyl azo-disperse dyes for dyeing polyester fabrics. Dyes and Pigments 2004;60:249–264.

[8] Mishra V, Jain MC. 2-Amino-4-phenl-5-phenylazothiazole as an analytical reagent for spectrophotometric determination of iron (III). J Indian Chem Soc 1988;65:883 – 884.

[9] Abdelhamid AO, Sayed AR, Zaki YH. Reaction of hydrazonoyl halides 51[1]: A facile synthesis of 5-arylthiazoles and triazolino[4,3-*a*]pyrimidines as antimicrobial agents. Phosphorus, Sulfur, and Silicon 2007;182: 1447–1457.

[10] Abdelhamid AO, Sayed AR. Reaction of Hydrazonoyl Halides 52:[1] Synthesis and antimicrobial activity of some new pyrazolines and 1,3,4-thiadiazolines. Phosphorus, Sulfur, and Silicon 2007;182:1767–1777.

[11] Abdelhamid AO, Ismail ZH, El Gendy MS, Ghorab MM, Reactions with hydrazonoyl Halides 53:[1] Synthesis and Antimicrobial Activity of Triazolino[4,3-*a*]pyrimidines and 5-Arylazothiazoles. Phosphorus, Sulfur, and Silicon 2007;182:2409–2418.

[12] Khalil AM, Berghot MA, Gouda MA, El Bialy SA. Synthesis and antibacterial studies of azodispersed dyes derived from 2-(thiazol-2-yl)phthalazine-1,4-diones. Monatsh Chem 2010;141:1353–1360.

[13] Ball P, Nichollst CH. Azo-hydrazone tautomerism of hydroxyazo compounds-a review. Dyes and Pigments 1982;3:5-26.

[14] Kim YD, Cho JH, Park CR, Choi J, Yoon C, Kim JP. Synthesis, application and investigation of structure–thermal stability relationships of thermally stable water-soluble azo naphthalene dyes for LCD red color filters. Dyes and Pigments 2011;89:1-8.

[15] Farrera J, Canal I, Hidalgo-Fernandez P, Perez-Garcia ML, Huertas O, Luque FJ. Towards a tunable tautomeric switch in azobenzene biomimetics: Implications for the binding affinity of 2-(4'-Hydroxyphenylazo)benzoic Acid to streptavidin. Chem Eur J 2008;14:2277–2285.

[16] Lee HY, Song X, Park H, Baik M, Lee D. Torsionally Responsive C_3-Symmetric Azo Dyes: Azo–hydrazone tautomerism, conformational switching, and application for chemical sensing. J Am Chem Soc 2010;132:12133–12144.

[17] Zhi-Gang Y, Chun-Xia Z, De-Feng Z, Freeman HS, Pei-Tong C, Jie H. Monoazo dyes based on 5,10-dihydrophenophosphazine, Part 2: Azo acid dyes. Dyes and Pigments 2009;81:137–143.

[18] Pavlovic G, Racane L, Cicak H, Tralic-Kulenovic V. The synthesis and structural study of two benzothiazolyl azo dyes: X-ray crystallographic and computational study of azo–hydrazone tautomerism. Dyes and Pigments 2009;83:354–362.

[19] Griffiths J, Lee WJ. Synthesis, light absorption and fluorescence properties of new thiazole analogues of the xanthene dyes. Dyes and Pigments 2003;57:107–114.

[20] a)Kodomari M, Suzuki M, Tanigawaa K, Aoyama T. A convenient and efficient method for the synthesis of mono and N,N-disubstituted thioureas. Tet Lett 2005;46:5841–5843.

b) Hartman VH, Inge R. Darstellung und Charakterisierung 1,l-disubstituierter Thioharnstoffe. Journal f. prakt. Chemi 1973;315:143-148.

[21] Habibi MH, Hassanzadeh A, Zeini-Isfahani A. Spectroscopic studies of Solophenyl red 3BL polyazo dye tautomerism in different solvents using UV–visible, ^{1}H NMR and steady-state fluorescence techniques. Dyes and Pigments, 2006;69:93-101.

[22] Frisch MJ, Trucks GW, Schlegel HB, Scuseria GE, Robb MA, Cheeseman JR, Scalmani G, Barone V, Mennucci B, Petersson GA, Nakatsuji H, Caricato, M, Li X, Hratchian HP, Izmaylov AF, Bloino J, Zheng G, Sonnenberg JL, Hada M, Ehara M, Toyota K, Fukuda R, Hasegawa J, Ishida M, Nakajima T, Honda Y, Kitao O, Nakai H, Vreven T, Montgomery JA Jr., Peralta JE, Ogliaro F, Bearpark M, Heyd J J, Brothers E, Kudin KN, Staroverov V N, Kobayashi R, Normand J, Raghavachari K, Rendell A, Burant JC, Iyengar SS, Tomasi J,

19

Cossi M, Rega N, Millam NJ, Klene M, Knox JE, Cross JB, Bakken V, Adamo C, Jaramillo J, Gomperts R, Stratmann RE, Yazyev O, Austin AJ, Cammi R, Pomelli C, Ochterski JW, Martin RL, Morokuma K, Zakrzewski VG, Voth, GA, Salvador P, Dannenberg JJ, Dapprich S, Daniels AD, Farkas O, Foresman JB, Ortiz JV, Cioslowski J, Fox DJ. Gaussian 09, revision C.01; Wallingford CT:Gaussian, Inc; 2010.

[23] Treutler O, Ahlrichs R. Efficient molecular numerical integration schemes. J Chem Phys 1995;102:346-354.

[24] Becke AD. A new mixing of Hartree–Fock and local density-functional theories J Chem Phys 1993;98: 1372-1377.

[25] Lee C, Yang W, Parr RG. Development of the Colle-Salvetti correlation-energy formula into a functional of the electron density. Phys Rev B 1988;37:785-789.

[26] (a) Hehre WJ, Radom L, Schleyer PvR, Pople , JA. Ab Initio Molecular Orbital Theory, New York: Wiley; 1986. (b) Bauernschmitt R, Ahlrichs R. Treatment of electronic excitations within the adiabatic approximation of time dependent density functional theory. Chem Phys Lett. 1996;256:454-464. (c) Furche F, Rappaport D. Density functional theory for excited states: Equilibrium structure and electronic spectra. In Computational Photochemistry, Olivucci, M, editor, Amsterdam: Elsevier; 2005;16: Chapter 3.

[27] Ebead YH. Spectrophotometric investigations and computational calculations of prototropic tautomerism and acide base properties of some new azo dyes. Dyes and Pigments 2011; 92: 705-13.

List of Tables:

Table 1

Experimental data for synthesis of dyes **8a-8e**

Dye	R	R'	R''	Yield %	M.P. (°C)	Thermal stability °C
8a	Cl	H	H	79	278-80	267
8b	F	H	H	26	>300	316
8c	NO_2	H	H	70	276-78	254
8d	H	H	NO_2	77	276-78	266
8e	NO_2	NO_2	H	45	270-72	264

Table 2

FT-IR, Mass, ^{1}H NMR data for dyes **8a-8e**
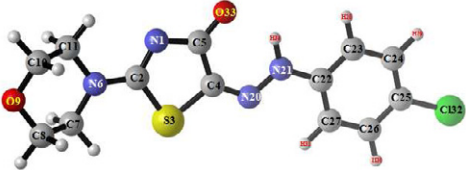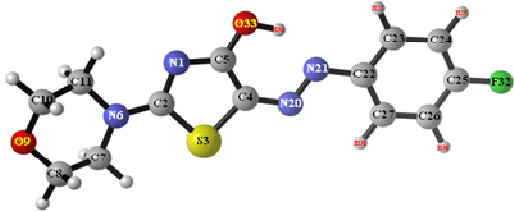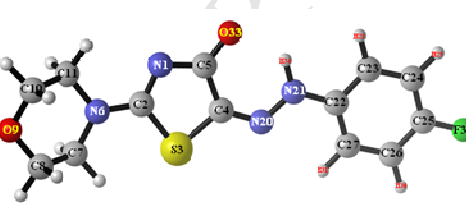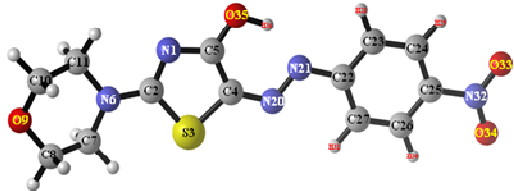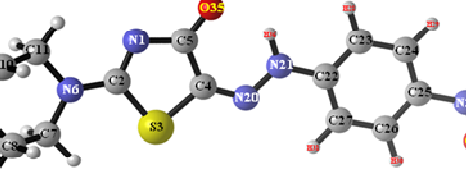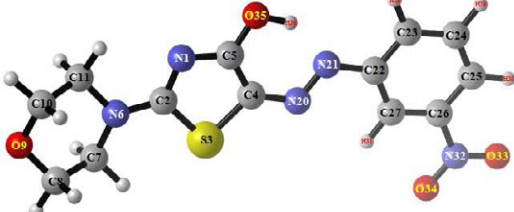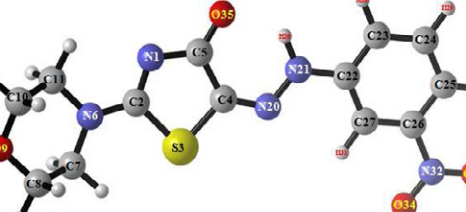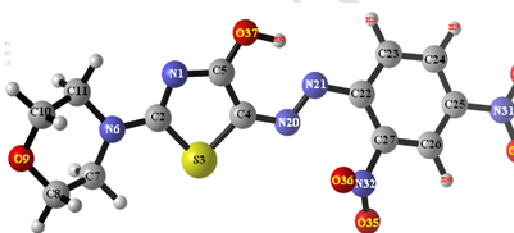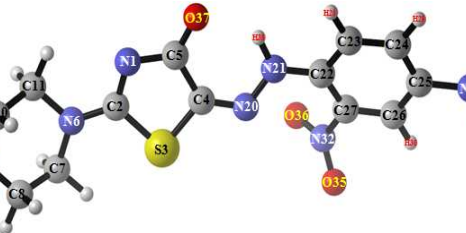
Dye	FT-IR υ_{max} (cm^{-1}, KBr)	Mass m/z M+1	^{1}H-NMR (ppm, DMSO-*d6*)
8a	1541(N=N), 1666 (C=O)	325.3	10.5 (1H, S, NH), 7.36 (2H, d, ArH, 8.8 Hz), 7.24 (2H, d, ArH, 8.8 Hz), 3.9 (2H, t, CH, 4.4,5.1 Hz), 3.7 (4H, m, CH, 4.8, 4.4 Hz), 3.6 (2H, m, CH)
8b	1558 (N=N), 1682 (C=O)	309.4	11.00 (1H, S, NH), 8.21 (2H,d, ArH, 9.5 Hz), 7.35 (2H, d, ArH, 9.2 Hz), 3.92 (2H, t, CH, 4.0,5.1 Hz), 3.75 (4H, m, CH), 3.62 (2H, t, CH, 5.1,4.0 Hz)
8c	1560 (N=N), 1649 (C=O)	336.4	10.4 (1H, s, NH), 7.2 (4H, m, ArH), 3.9 (2H, t, CH, 4.4,5.1 Hz), 3.7 (4H, m, CH), 3.5 (2H, t, CH, 4.8,4.0 Hz)
8d	1556 (N=N), 1677 (C=O)	336.4	14 (1H, s, OH), 10.4(1H, s, NH), 8.17 (1H, dd, ArH, 7.7 Hz), 7.77-7.79 (2H, m, ArH), 7.14 (1H, m, ArH), 3.94 (2H,t, CH, 4.4, 4.8 Hz), 3.75 (4H, m, CH), 3.63 (2H, t, CH, 5.1,4.0 Hz)
8e	1571 (N=N), 1691 (C=O)	381.3	10.74 (1H, S, NH), 8.85 (1H, d, ArH, 1.5 Hz), 8.53 (1H, d, ArH, 9.5 Hz), 7.93 (1H, d, ArH, 9.1 Hz), 3.95 (2H, t, CH,4.4, 5.1 Hz), 3.74 (4H, m, CH), 3.67 (2H, t, CH, 5.5 Hz)

Table 3

Photo-physical properties of dyes **8a-8e**

Dye	λ_{max} (nm)	Molar Extinction co-efficient ($dm^3\,mol^{-1}\,cm^{-1}$)
8a	371(299)	22305(8636.)
8b	406, 565 (304)	37723, 14338 (9138)
8c	368(299)	28328 (13278)
8d	344, 425(281)	12742, 14348 (9799)
8e	535(268)	54981 (11597)

Table 4

Ground state optimized structures of dyes **8a-8e** in their azo and hydrazone tautomeric forms.

Comp	Azo	Hydrazone
8a		
8b		
8c		
8d		
8e		

Table 5

Computed interatomic distances of azo-hydrazone tautomers of dye **8a** in Å

Interatomic distance	B3LYP/6-31G(d)		B3LYP/6-311++G(d,p)	
	Azo	Hydrazone	Azo	Hydrazone
N1-C2	1.323	1.309	1.322	1.308
C2-S3	1.776	1.801	1.772	1.796
S3-C4	1.775	1.783	1.773	1.781
C4-C5	1.410	1.494	1.407	1.494
C5-N1	1.348	1.378	1.345	1.374
C4-N20	1.341	1.292	1.339	1.288
N20-N21	1.294	1.329	1.289	1.327
N21-C22	1.404	1.395	1.405	1.397
C27-C22	1.407	1.403	1.405	1.400
C25-Cl32	1.759	1.760	1.759	1.760
C5-O33	1.320	1.234	1.318	1.229
O33-H34	1.011	1.904	1.006	1.923
N21-H34	1.732	1.024	1.729	1.023

Table 6

Computed energy in gas phase for dyes **8a-8e** using B3LYP functional**.**

Dye	Azo			Hydrazone		
6-31 G(d)	E/Hartree[a]	ΔE/kJ[b] mol $^{-1}$	ΔG/Hartree[c]	E/Hartree[a]	ΔE/kJ[b] mol $^{-1}$	ΔG/Hartree[c]
8a	-1731.00	50.40	-1730.79	-1731.02	0	-1730.81
8b	-1370.64	49.06	-1370.43	-1370.66	0	-1370.45
8c	-1475.91	53.27	-1475.69	-1475.93	0	-1475.71
8d	-1475.91	50.54	-1475.69	-1475.93	0	-1475.71
8e	-1680.39	46.77	-1680.18	-1680.41	0	-1680.19
6-311 ++G(d,p)						
8a	-1731.29	44.98	-1731.09	-1731.31	0	-1731.10
8b	-1370.94	43.80	-1370.73	-1370.96	0	-1370.75
8c	-1476.24	47.86	-1476.02	-1476.26	0	-1476.04
8d	-1476.23	45.02	-1476.02	-1476.25	0	-1476.04
8e	-1680.79	40.80	-1680.57	-1680.80	0	-1680.59

1 Hartree = 2626 kJ/mol

[a]Calculated energies, [b]Gibbs free energies, [c]relative energies.

7

Table 7

Computed energy in DMF for dyes **8a-8e** using B3LYP functional.

Dye	Azo			Hydrazone		
6-31G(d)	E/Hartree[a]	$\Delta E/kJ$[b] mol^{-1}	ΔG/Hartree[c]	E/Hartree[a]	$\Delta E/kJ$[b] mol^{-1}	ΔG/Hartree[c]
8a	-1731.00	50.4	-1730.79	-1731.02	0	-1730.81
8b	-1370.64	49.00	-1370.43	-1370.66	0	-1370.45
8c	-1475.91	53.89	-1475.69	-1475.93	0	-1475.71
8d	-1475.69	50.66	-1476.00	-1475.93	0	-1475.71
8e	-1680.39	47.70	-1680.18	-1680.41	0	-1680.19
6-311 ++G(d,p)						
8a	-1731.29	44.79	-1731.09	-1731.31	0	-1731.1
8b	-1370.94	43.49	-1370.73	-1370.96	0	-1370.75
8c	-1476.24	48.62	-1476.02	-1476.25	0	-1476.04
8d	-1476.23	45.01	-1476.02	-1476.25	0	-1476.04
8e	-1680.78	42.02	-1680.57	-1680.80	0	-1680.59

1 Hartree = 2626 kJ/mol

[a]Calculated energies, [b]Gibbs free energies, [c]relative energies.

List of Tables (Supporting Information)

Table 21. Observed UV-visible absorption and computed absorption in DMF at CAM-B3LYP/6-31G(d) for dyes **8a-8e**.

Table 22. Observed UV-visible absorption and computed absorption in DMF at M06/6-31G(d) for dyes **8a-8e**.

Table 23. Observed UV-visible absorption and computed absorption in DMF at B3LYP/6-311++G(d,p) for dyes **8a-8e**.

Table 24. Observed UV-visible absorption and computed absorption in DMF at CAM-B3LYP/6-311++G(d,p) for dyes **8a-8e**.

Table 25. Observed UV-visible absorption and computed absorption in DMF at M06/6-311++G(d,p) for dyes **8a-8e**.

Table 26. Observed UV-visible absorption and computed absorption in gas phase at B3LYP/6-31G(d) for dyes **8a-8e**.

Table 27. Observed UV-visible absorption and computed absorption in gas phase at CAM-B3LYP/6-31G(d) for dyes **8a-8e**.

Table 28. Observed UV-visible absorption and computed absorption in gas phase at M06/6-31G(d) for dyes **8a-8e**.

Table 29. Observed UV-visible absorption and computed absorption in gas phase at B3LYP/6-311++G(d,p) for dyes **8a-8e**.

Table 30. Observed UV-visible absorption and computed absorption in gas phase at CAM- B3LYP/6-311++G(d,p) for dyes **8a-8e**.

Table 31. Observed UV-visible absorption and computed absorption in gas phase at M06/6-311++G(d,p) for dyes **8a-8e**.

Table 1

Ground state optimized structures of dyes **8a-8e** in their azo and hydrazone tautomeric forms at B3LYP/6-311++G(d,p) level of computation.

Comp	Azo	Hydrazone
8a		
8b		
8c		
8d		
8e		

Table 2

Computed interatomic distances of azo-hydrazone tautomers of dye **8a** in Å.

Interatomic distance	CAM B3LYP/6-31G(d)		CAM B3LYP/6-311++G(d,p)	
	Azo	Hydrazone	Azo	Hydrazone
N1-C2	1.317	1.304	1.315	1.303
C2-S3	1.761	1.786	1.756	1.781
S3-C4	1.763	1.772	1.761	1.771
C4-C5	1.400	1.491	1.397	1.491
C5-N1	1.346	1.373	1.343	1.369
C4-N20	1.342	1.282	1.340	1.278
N20-N21	1.278	1.323	1.272	1.321
N21-C22	1.409	1.394	1.409	1.396
C27-C22	1.398	1.395	1.396	1.392
C25-Cl32	1.748	1.749	1.747	1.749
C5-O33	1.313	1.226	1.311	1.221
O33-H34	1.005	1.895	1.001	1.913
N21-H34	1.734	1.022	1.729	1.020

Table 3

Computed interatomic distances of azo-hydrazone tautomers of dye **8a** in Å.

Interatomic distance	M06/6-31G(d)		M06/6-311++G(d,p)	
	Azo	Hydrazone	Azo	Hydrazone
N1-C2	1.318	1.303	1.315	1.301
C2-S3	1.764	1.791	1.759	1.785
S3-C4	1.768	1.777	1.765	1.774
C4-C5	1.406	1.491	1.403	1.491
C5-N1	1.343	1.373	1.339	1.369
C4-N20	1.339	1.286	1.337	1.282
N20-N21	1.285	1.323	1.279	1.319
N21-C22	1.403	1.393	1.403	1.392
C27-C22	1.401	1.396	1.398	1.393
C25-Cl32	1.749	1.750	1.746	1.747
C5-O33	1.313	1.226	1.309	1.220
O33-H34	1.002	1.907	0.997	1.916
N21-H34	1.775	1.026	1.773	1.025

Table 4

Computed interatomic distances of azo-hydrazone tautomers of dye **8b** in Å.

Interatomic distance	B3LYP/6-31G(d)		B3LYP/6-311++G(d,p)	
	Azo	Hydrazone	Azo	Hydrazone
N1-C2	1.322	1.309	1.321	1.308
C2-S3	1.776	1.800	1.772	1.795
S3-C4	1.775	1.783	1.773	1.782
C4-C5	1.408	1.491	1.406	1.492
C5-N1	1.350	1.379	1.346	1.374
C4-N20	1.344	1.293	1.341	1.288
N20-N21	1.292	1.327	1.287	1.325
N21-C22	1.406	1.399	1.407	1.399
C22-C23	1.404	1.403	1.402	1.401
C27-C22	1.408	1.403	1.405	1.400
C25-F32	1.350	1.352	1.357	1.358
C5-O33	1.322	1.234	1.319	1.229
O33-H34	1.010	1.907	1.005	1.924
N21-H34	1.740	1.024	1.736	1.023

Table 5

14

Computed interatomic distances of azo-hydrazone tautomers of dye **8b** in Å.

Interatomic distance	CAM B3LYP/6-31G(d)		CAM B3LYP/6-311++G(d,p)	
	Azo	Hydrazone	Azo	Hydrazone
N1-C2	1.316	1.304	1.314	1.303
C2-S3	1.760	1.785	1.756	1.781
S3-C4	1.762	1.773	1.761	1.771
C4-C5	1.397	1.489	1.395	1.490
C5-N1	1.348	1.374	1.344	1.369
C4-N20	1.346	1.283	1.342	1.278
N20-N21	1.276	1.321	1.270	1.320
N21-C22	1.410	1.398	1.411	1.398
C22-C23	1.395	1.396	1.393	1.394
C27-C22	1.399	1.395	1.396	1.393
C25-F32	1.343	1.345	1.350	1.352
C5-O33	1.315	1.226	1.312	1.221
O33-H34	1.004	1.897	1.000	1.913
N21-H34	1.743	1.022	1.738	1.020

Table 6

Computed interatomic distances of azo-hydrazone tautomers of dye **8b** in Å.

Interatomic distance	M06/6-31G(d)		M06/6-311++G(d,p)	
	Azo	Hydrazone	Azo	Hydrazone
N1-C2	1.317	1.303	1.314	1.300
C2-S3	1.764	1.791	1.759	1.785
S3-C4	1.768	1.777	1.765	1.774
C4-C5	1.404	1.489	1.401	1.489
C5-N1	1.344	1.374	1.340	1.369
C4-N20	1.342	1.287	1.339	1.282
N20-N21	1.283	1.320	1.277	1.318
N21-C22	1.404	1.396	1.404	1.395
C22-C23	1.398	1.397	1.395	1.394
C27-C22	1.401	1.396	1.398	1.393
C25-F32	1.337	1.338	1.340	1.342
C5-O33	1.314	1.226	1.310	1.220
O33-H34	1.001	1.909	0.996	1.919
N21-H34	1.777	1.026	1.775	1.024

Table 7

Computed interatomic distances of azo-hydrazone tautomers of dye **8c** in Å.

Interatomic distance	B3LYP/6-31G(d)		B3LYP/6-311++G(d,p)	
	Azo	Hydrazone	Azo	Hydrazone
N1-C2	1.327	1.311	1.325	1.309
C2-S3	1.778	1.803	1.774	1.798
S3-C4	1.776	1.781	1.774	1.779
C4-C5	1.419	1.501	1.417	1.501
C5-N1	1.344	1.374	1.340	1.370
C4-N20	1.333	1.289	1.329	1.285
N20-N21	1.301	1.336	1.297	1.334
N21-C22	1.398	1.386	1.398	1.386
C22-C23	1.408	1.408	1.406	1.406
C27-C22	1.411	1.408	1.409	1.405
C25-N32	1.462	1.459	1.468	1.465
N32-O33	1.234	1.234	1.228	1.228
N32-O34	1.234	1.234	1.228	1.228
C5-O35	1.316	1.233	1.312	1.227
O35-H36	1.015	1.897	1.011	1.912
N21-H36	1.711	1.025	1.700	1.023

Table 8

Computed interatomic distances of azo-hydrazone tautomers of dye **8c** in Å.

Interatomic distance	CAM B3LYP/6-31G(d)		CAM B3LYP/6-311++G(d,p)	
	Azo	Hydrazone	Azo	Hydrazone
N1-C2	1.320	1.305	1.319	1.304
C2-S3	1.762	1.788	1.758	1.783
S3-C4	1.764	1.771	1.763	1.769
C4-C5	1.408	1.497	1.406	1.498
C5-N1	1.342	1.370	1.338	1.365
C4-N20	1.333	1.279	1.329	1.275
N20-N21	1.285	1.330	1.280	1.329
N21-C22	1.403	1.385	1.403	1.385
C22-C23	1.399	1.401	1.397	1.399
C27-C22	1.402	1.400	1.399	1.397
C25-N32	1.460	1.457	1.467	1.463
N32-O33	1.223	1.224	1.217	1.218
N32-O34	1.223	1.224	1.217	1.218
C5-O35	1.309	1.225	1.306	1.219
O35-H36	1.010	1.888	1.007	1.903
N21-H36	1.709	1.022	1.696	1.021

Table 9

Computed interatomic distances of azo-hydrazone tautomers of dye **8c** in Å.

Interatomic distance	M06/6-31G(d)		M06/6-311++G(d,p)	
	Azo	Hydrazone	Azo	Hydrazone
N1-C2	1.321	1.305	1.319	1.302
C2-S3	1.765	1.794	1.760	1.788
S3-C4	1.770	1.774	1.767	1.771
C4-C5	1.412	1.497	1.411	1.498
C5-N1	1.338	1.370	1.334	1.366
C4-N20	1.330	1.283	1.326	1.279
N20-N21	1.292	1.330	1.287	1.327
N21-C22	1.397	1.383	1.396	1.382
C22-C23	1.402	1.402	1.399	1.400
C27-C22	1.404	1.401	1.401	1.398
C25-N32	1.460	1.457	1.467	1.464
N32-O33	1.223	1.223	1.216	1.216
N32-O34	1.223	1.223	1.216	1.216
C5-O35	1.309	1.225	1.304	1.218
O35-H36	1.005	1.902	1.000	1.907
N21-H36	1.758	1.026	1.749	1.025

19

Table 10

Computed interatomic distances of azo-hydrazone tautomers of dye **8d** in Å.

Interatomic distance	B3LYP/6-31G(d)		B3LYP/6-311++G(d,p)	
	Azo	Hydrazone	Azo	Hydrazone
N1-C2	1.326	1.311	1.325	1.309
C2-S3	1.777	1.802	1.772	1.797
S3-C4	1.776	1.781	1.774	1.780
C4-C5	1.415	1.498	1.412	1.498
C5-N1	1.345	1.375	1.341	1.371
C4-N20	1.336	1.290	1.333	1.285
N20-N21	1.297	1.333	1.292	1.331
N21-C22	1.404	1.392	1.404	1.393
C22-C23	1.406	1.406	1.403	1.404
C27-C22	1.405	1.401	1.403	1.398
C26-N32	1.476	1.476	1.484	1.484
N32-O33	1.231	1.231	1.225	1.225
N32-O34	1.230	1.230	1.224	1.224
C5-O35	1.318	1.234	1.315	1.228
O35-H36	1.012	1.896	1.007	1.913
N21-H36	1.723	1.024	1.717	1.023

Table 11

Computed interatomic distances of azo-hydrazone tautomers of dye **8d** in Å.

Interatomic distance	CAM B3LYP/6-31G(d)		CAM B3LYP/6-311++G(d,p)	
	Azo	Hydrazone	Azo	Hydrazone
N1-C2	1.319	1.305	1.318	1.304
C2-S3	1.761	1.787	1.757	1.782
S3-C4	1.763	1.771	1.762	1.770
C4-C5	1.404	1.495	1.402	1.496
C5-N1	1.343	1.370	1.339	1.366
C4-N20	1.336	1.280	1.333	1.275
N20-N21	1.281	1.327	1.276	1.326
N21-C22	1.407	1.390	1.407	1.391
C22-C23	1.397	1.398	1.394	1.396
C27-C22	1.396	1.394	1.394	1.391
C26-N32	1.470	1.471	1.478	1.479
N32-O33	1.222	1.222	1.216	1.215
N32-O34	1.221	1.221	1.215	1.215
C5-O35	1.311	1.226	1.308	1.220
O35-H36	1.007	1.888	1.003	1.904
N21-H36	1.723	1.022	1.714	1.021

Table 12

Computed interatomic distances of azo-hydrazone tautomers of dye **8d** in Å.

Interatomic distance	M06/6-31G(d)		M06/6-311++G(d,p)	
	Azo	Hydrazone	Azo	Hydrazone
N1-C2	1.320	1.305	1.318	1.302
C2-S3	1.764	1.792	1.758	1.786
S3-C4	1.770	1.775	1.767	1.772
C4-C5	1.410	1.495	1.408	1.495
C5-N1	1.340	1.371	1.336	1.366
C4-N20	1.334	1.283	1.330	1.278
N20-N21	1.288	1.327	1.282	1.324
N21-C22	1.402	1.390	1.401	1.389
C22-C23	1.399	1.399	1.396	1.397
C27-C22	1.398	1.394	1.396	1.392
C26-N32	1.473	1.473	1.482	1.481
N32-O33	1.221	1.220	1.214	1.213
N32-O34	1.220	1.220	1.213	1.213
C5-O35	1.311	1.225	1.307	1.219
O35-H36	1.003	1.922	0.998	1.928
N21-H36	1.767	1.025	1.759	1.024

Table 13

Computed interatomic distances of azo-hydrazone tautomers of dye **8e** in Å.

Interatomic distance	B3LYP/6-31G(d)		B3LYP/6-311++G(d,p)	
	Azo	Hydrazone	Azo	Hydrazone
N1-C2	1.331	1.313	1.330	1.311
C2-S3	1.777	1.804	1.773	1.799
S3-C4	1.776	1.777	1.774	1.775
C4-C5	1.426	1.506	1.424	1.507
C5-N1	1.339	1.370	1.334	1.366
C4-N20	1.324	1.286	1.320	1.281
N20-N21	1.307	1.342	1.303	1.341
N21-C22	1.386	1.376	1.385	1.376
C22-C23	1.411	1.412	1.409	1.410
C27-C22	1.419	1.415	1.415	1.410
C25-N31	1.463	1.462	1.469	1.468
N31-O33	1.232	1.232	1.226	1.226
N31-O34	1.232	1.231	1.226	1.226
C27-N32	1.474	1.473	1.481	1.480
N32-O35	1.229	1.229	1.222	1.221
N32-O36	1.228	1.227	1.222	1.221
C5-O37	1.314	1.233	1.311	1.227
O37-H38	1.013	1.873	1.008	1.888
N21-H38	1.716	1.026	1.712	1.025

23

Table 14

Computed interatomic distances of azo-hydrazone tautomers of dye **8e** in Å.

Interatomic distance	CAM B3LYP/6-31G(d)		CAM B3LYP/6-311++G(d,p)	
	Azo	Hydrazone	Azo	Hydrazone
N1-C2	1.325	1.307	1.325	1.307
C2-S3	1.761	1.789	1.757	1.784
S3-C4	1.76	1.767	1.763	1.765
C4-C5	1.416	1.503	1.415	1.504
C5-N1	1.336	1.366	1.331	1.361
C4-N20	1.322	1.276	1.317	1.271
N20-N21	1.293	1.338	1.290	1.337
N21-C22	1.390	1.374	1.389	1.373
C22-C23	1.402	1.405	1.400	1.403
C27-C22	1.407	1.406	1.404	1.401
C25-N31	1.461	1.459	1.467	1.465
N31-O33	1.222	1.222	1.216	1.216
N31-O34	1.222	1.222	1.216	1.216
C27-N32	1.468	1.467	1.474	1.473
N32-O35	1.220	1.220	1.213	1.213
N32-O36	1.219	1.218	1.213	1.212
C5-O37	1.306	1.225	1.303	1.220
O37-H38	1.009	1.868	1.006	1.882
N21-H38	1.706	1.023	1.695	1.022

Table 15

Computed interatomic distances of azo-hydrazone tautomers of dye **8e** in Å.

Interatomic distance	M06/6-31G(d)		M06/6-311++G(d,p)	
	Azo	Hydrazone	Azo	Hydrazone
N1-C2	1.326	1.307	1.220	1.304
C2-S3	1.764	1.794	1.759	1.790
S3-C4	1.770	1.771	1.767	1.768
C4-C5	1.421	1.503	1.419	1.503
C5-N1	1.333	1.366	1.329	1.503
C4-N20	1.320	1.280	1.316	1.275
N20-N21	1.299	1.337	1.295	1.335
N21-C22	1.383	1.373	1.383	1.372
C22-C23	1.405	1.406	1.402	1.402
C27-C22	1.412	1.409	1.406	1.403
C25-N31	1.461	1.460	1.468	1.466
N31-O33	1.222	1.222	1.214	1.214
N31-O34	1.221	1.221	1.214	1.214
C27-N32	1.471	1.470	1.477	1.476
N32-O35	1.219	1.219	1.210	1.210
N32-O36	1.218	1.217	1.211	1.210
C5-O37	1.306	1.224	1.302	1.218
O37-H38	1.004	1.888	0.998	1.896
N21-H38	1.759	1.027	1.754	1.026

Table 16

Computed energy in gas phase for dyes **8a-8e** using CAM-B3LYP functional**.**

Dye	Azo			Hydrazone		
6-31G(d)	E/Hartree[a]	ΔE/kJ[b] mol^{-1}	ΔG/Hartree[c]	E/Hartree[a]	ΔE/kJ[b] mol^{-1}	ΔG/Hartree[c]
8a	-1730.57	50.73	-1730.36	-1730.59	0	-1730.38
8b	-1370.18	50.80	-1369.97	-1370.20	0	-1369.99
8c	-1475.41	56.43	-1475.19	-1475.43	0	-1475.21
8d	-1475.41	53.06	-1475.18	-1475.43	0	-1475.20
8e	-1679.83	50.42	-1679.61	-1679.85	0	-1679.63
6-311 ++G(d,p)						
8a	-1730.86	47.30	-1730.65	-1730.88	0	-1730.67
8b	-1370.49	45.64	-1370.28	-1370.51	0	-1370.29
8c	-1475.74	51.18	-1475.52	-1475.76	0	-1475.54
8d	-1475.74	47.73	-1475.52	-1475.76	0	-1475.54
8e	-1680.23	44.90	-1680.01	-1680.24	0	-1680.02

1 Hartree = 2626 kJ/mol

[a]Calculated energies, [b]Gibbs free energies, [c]relative energies.

26

Table 17

Computed energy in DMF for dyes **8a-8e** using CAM-B3LYP functional.

Dye	Azo			Hydrazone		
6-31G(d)	E/Hartree[a]	ΔE/kJ[b] mol^{-1}	ΔG/Hartree[c]	E/Hartree[a]	ΔE/kJ[b] mol^{-1}	ΔG/Hartree[c]
8a	-1730.58	59.82	-1730.37	-1730.60	0	-1730.39
8b	-1370.20	57.97	-1369.98	-1370.22	0	-1370.00
8c	-1475.42	63.03	-1475.20	-1475.45	0	-1475.22
8d	-1475.42	59.65	-1475.20	-1475.44	0	-1475.22
8e	-1679.85	56.11	-1679.63	-1679.87	0	-1679.65
6-311 ++G(d,p)						
8a	-1730.88	56.70	-1730.67	-1730.90	0	-1730.69
8b	-1370.50	55.22	-1370.29	-1370.52	0	-1370.31
8c	-1475.76	59.90	-1475.54	-1475.78	0	-1475.56
8d	-1475.76	56.42	-1475.54	-1475.78	0	-1475.56
8e	-1680.25	52.28	-1680.03	-1680.27	0	-1680.05

1 Hartree = 2626 kJ/mol

[a]Calculated energies, [b]Gibbs free energies, [c]relative energies.

27

Table 18

Computed energy in gas phase for dyes **8a-8e** using M06 functional.

Dye	Azo			Hydrazone		
6-31 G(d)	E/Hartree[a]	$\Delta E/kJ$[b] mol^{-1}	$\Delta G/Hartree$[c]	E/Hartree[a]	$\Delta E/kJ$[b] mol^{-1}	$\Delta G/Hartree$[c]
8a	-1730.37	51.83	-1730.17	-1730.39	0	-1730.19
8b	-1370.02	50.24	-1369.81	-1370.03	0	-1369.82
8c	-1475.22	55.13	-1475.00	-1475.24	0	-1475.02
8d	-1475.22	52.09	-1475.00	-1475.24	0	-1475.02
8e	-1679.62	47.80	-1679.41	-1679.64	0	-1679.42
6-311 ++G(d,p)						
8a	-1730.64	44.79	-1730.43	-1730.65	0	-1730.45
8b	-1370.28	43.49	-1370.07	-1370.30	0	-1370.09
8c	-1475.51	48.63	-1475.30	-1475.53	0	-1475.32
8d	-1475.51	45.02	-1475.30	-1475.53	0	-1475.32
8e	-1679.97	42.02	-1679.76	-1679.99	0	-1679.77

1 Hartree = 2626 kJ/mol

[a]Calculated energies, [b]Gibbs free energies, [c]relative energies.

28

Table 19

Computed energy in DMF for dyes **8a-8e** using M06 functional.

Dye	Azo			Hydrazone		
6-31G(d)	E/Hartree[a]	ΔE/kJ[b] mol^{-1}	ΔG/Hartree[c]	E/Hartree[a]	ΔE/kJ[b] mol^{-1}	ΔG/Hartree[c]
8a	-1730.39	58.45	-1730.18	-1730.41	0	-1730.20
8b	-1370.03	56.99	-1369.82	-1370.05	0	-1369.84
8c	-1475.24	60.73	-1475.02	-1475.26	0	-1475.04
8d	-1475.24	58.30	-1475.02	-1475.26	0	-1475.04
8e	-1679.64	52.15	-1679.43	-1679.66	0	-1679.45
6-311 ++G(d,p)						
8a	-1730.65	54.97	-1730.44	-1730.67	0	-1730.46
8b	-1370.30	53.81	-1370.09	-1370.32	0	-1370.11
8c	-1475.53	57.31	-1475.32	-1475.55	0	-1475.34
8d	-1475.53	54.76	-1475.32	-1475.55	0	-1475.33
8e	-1679.99	48.44	-1679.78	-1680.01	0	-1679.80

1 Hartree = 2626 kJ/mol

[a]Calculated energies, [b]Gibbs free energies, [c]relative energies.

29

Table 20

Observed UV-visible absorption and computed absorption in DMF at B3LYP/6-31G(d) for dyes **8a-8e**.

Dye	λ_{max} [a] (nm)	TD-DFT					
		Azo			Hydrazone		
		Vertical [b] Excitation (nm)	f [c]	Orbital Contribution Band gap (eV)	Vertical [b] Excitation (nm)	f [c]	Orbital Contribution Band gap (eV)
8a	371 299	434	1.122	H→L (0.710)	390 288	0.894 0.167	H→L (0.707) H-1→L (0.638)
8b	406 304 565	429	1.023	H→L (0.710)	391 286	0.803 0.163	H→L (0.707) H-1→L (0.632)
8c	368 299	482	1.285	H→L (0.710)	414	1.173	H→L (0.703)
8d	425 281 344	428	1.060	H→L+1 (0.706)	375 291	0.879 0.168	H→L+1 (0.705) H-1 →L+1 (0.668)
8e	535 268	498 432	0.968 0.205	H→L (0.685) H→L+1 (0.667)	432 391	0.627 0.394	H→L (0.641) H→L+1 (0.629)

[a]Experimental absorption wavelength, [b]Computed absorption wavelength, [c]Oscillator strength

30

Table 21

Observed UV-visible absorption and computed absorption in DMF at CAM-B3LYP/6-31G(d) for dyes
8a-8e.

Dye	λ_{max} [a] (nm)	TD-DFT					
		Azo			Hydrazone		
		Vertical [b] Excitation (nm)	f [c]	Orbital Contribution Band gap (eV)	Vertical [b] Excitation (nm)	f [c]	Orbital Contribution Band gap (eV)
8a	371 299	400	1.1196	H→L (0.699)	342 253	0.9908 0.1214	H→L (0.692) H-1→L (0.417)
8b	406 304 565	395	1.0217	H→L (0.700)	344 251	0.8874 0.3054	H→L (0.694) H-1→L (0.505)
8c	368 299	427	1.3085	H→L (0.679)	354 258	1.277 0.2242	H→L(0.671) H-1→L (0.440)
8d	425 281 344	397	1.0557	H→L+1 (0.528)	334 254	0.930 0.295	H→L+1(0.667) H-1→L+1(0.568)
8e	535 268	435 329	1.1147 0.1708	H→L (0.672) H→L +1 (0.539)	360 312	0.8511 0.331	H→L (0.641) H→L+1(0.375)

[a]Experimental absorption wavelength, [b]Computed absorption wavelength, [c]Oscillator strength

Table 22

Observed UV-visible absorption and computed absorption in DMF at M06/6-31G(d) for dyes **8a-8e**.

Dye	λ_{max}[a] (nm)	TD-DFT					
		Azo			Hydrazone		
		Vertical[b] Excitation (nm)	f[c]	Orbital Contribution Band gap (eV)	Vertical[b] Excitation (nm)	f[c]	Orbital Contribution Band gap (eV)
8a	371 299	428	1.104	H→L (0.707)	378 266	0.902 0.134	H→L (0.705) H-1→L (0.534)
8b	406 304 565	422	0.998	H→L (0.708)	379 263	0.804 0.146	H→L (0.706) H-1→L (0.533)
8c	368 299	467	1.278	H→L (0.706)	396 291	1.181 0.119	H→L(0.696) H-1→L (0.617)
8d	425 281 344	421	1.028	H→L+1 (0.697)	363 277	0.871 0.196	H→L+1(0.704) H-1→L+1(0.589)
8e	535 268	479	1.002	H→L (0.684)	409 363	0.707 0.347	H→L (0.657) H→L+1(0.637)

[a]Experimental absorption wavelength, [b]Computed absorption wavelength, [c]Oscillator strength.

32

Table 23

Observed UV-visible absorption and computed absorption in DMF at B3LYP/6-311++G(d,p) for dyes **8a-8e**.

Dye	λ_{max} [a] (nm)	TD-DFT					
		Azo			Hydrazone		
		Vertical [b] Excitation (nm)	f [c]	Orbital Contribution Band gap (eV)	Vertical [b] Excitation (nm)	f [c]	Orbital Contribution Band gap (eV)
8a	371 299	445	1.110	H→L (0.709)	404 293	0.894 0.144	H→L (0.706) H-1→L (0.421)
8b	406 304 565	439	1.008	H→L (0.709)	397 290	0.816 0.161	H→L (0.706) H-1→L (0.578)
8c	368 299	506	1.293	H→L (0.709)	435	1.145	H→L (0.702)
8d	425 281 344	438	1.056	H→L+1 (0.707)	383 294	0.889 0.186	H→L+1 (0.705) H-1→L+1 (0.645)
8e	535 268	517 469	0.915 0.282	H→L (0.661) H→L+1 (0.648)	452 418 333	0.467 0.524 0.192	H→L (0.562) H→L+1 (0.555) H→L+2 (0.659)

[a]Experimental absorption wavelength, [b]Computed absorption wavelength, [c]Oscillator strength

33

Table 24

Observed UV-visible absorption and computed absorption in DMF at CAM-B3LYP/6-311++G(d,p) for dyes **8a-8e**.

| Dye | λ_{max}[a] (nm) | TD-DFT | | | | | |
| | | Azo | | | Hydrazone | | |
		Vertical[b] Excitation (nm)	f[c]	Orbital Contribution Band gap (eV)	Vertical[b] Excitation (nm)	f[c]	Orbital Contribution Band gap (eV)
8a	371 299	409	1.1076	H→L (0.698)	351 257	0.9813 0.3051	H→L (0.691) H-1→L (0.431)
8b	406 304 565	404	1.0083	H→L (0.699)	350 256	0.8827 0.2969	H→L (0.693) H-1→L (0.479)
8c	368 299	442	1.3393	H→L (0.672)	367 262	1.2895 0.2548	H→L(0.662) H-1→L (0.399)
8d	425 281 344	407	1.0343	H→L+1 (0.698)	340 258	0.9460 0.3265	H→L+1(0.685) H-1→L+1(0.521)
8e	535 268	445 353	1.1759 0.1609	H→L (0.665) H→L +1 (0.579)	369 328	0.8189 0.4410	H→L (0.607) H→L+1(0.481)

[a]Experimental absorption wavelength, [b]Computed absorption wavelength, [c]Oscillator strength

Table 25

Observed UV-visible absorption and computed absorption in DMF at M06/6-311++G(d,p) for dyes **8a-8e**.

Dye	λ_{max} [a] (nm)	TD-DFT					
		Azo			Hydrazone		
		Vertical [b] Excitation (nm)	f [c]	Orbital Contribution Band gap (eV)	Vertical [b] Excitation (nm)	f [c]	Orbital Contribution Band gap (eV)
8a	371 299	438	1.088	H→L (0.706)	387 269	0.898 0.206	H→L (0.704) H-1→L (0.644)
8b	406 304 565	431	0.981	H→L (0.707)	384 266	0.806 0.175	H→L (0.705) H-1→L (0.596)
8c	368 299	487	1.283	H→L (0.704)	413 297	1.162 0.107	H→L(0.694) H-1→L (0.528)
8d	425 281 344	431	1.011	H→L+1 (0.699)	371 280	0.870 0.205	H→L+1(0.703) H-1→L+1(0.535)
8e	535 268	492	1.045	H→L (0.682)	421 386	0.633 0.406	H→L (0.610) H→L+1(0.594)

[a]Experimental absorption wavelength, [b]Computed absorption wavelength, [c]Oscillator strength

Table 26

Observed UV-visible absorption and computed absorption in gas phase at B3LYP/6-31G(d) for dyes **8a-8e**.

Dyes	λ_{max} [a] (nm)	TD-DFT					
		Azo			Hydrazone		
		Vertical [b] Excitation (nm)	f [c]	Orbital contribution band gap (eV)	Vertical [b] Excitation (nm)	f [c]	Orbital Contribution Band gap (eV)
8a	371 299	410	0.991	H→L (0.605)	380	0.733	H→L (0.637)
8b	406 304 565	404	0.899	H→L (0.603)	346	0.588	H→L (0.647)
8c	368 299	431	1.107	H →L (0.608)	383 293	0.994 0.110	H→L (0.639) H-1→L (0.604)
8d	425 281 344	402 380	0.927 0.844	H→L (0.603)	363 283	0.724 0.113	H→L+1 (0.633) H-1→L+1 (0.479)
8e	535 268	448 415	0.770 0.102	H→L (0.579) H-1→L (0.626)	397 354	0.632 0.265	H→L (0.614) H→L+1 (0.610)

[a]Experimental absorption wavelength, [b]Computed absorption wavelength, [c]Oscillator strength

Table 27

Observed UV-visible absorption and computed absorption in gas phase at CAM-B3LYP/6-31G(d) for dyes **8a-8e**.

Dyes	λ_{max}[a] (nm)	TD-DFT					
		Azo			Hydrazone		
		Vertical[b] Excitation (nm)	f[c]	Orbital contribution band gap (eV)	Vertical[b] Excitation (nm)	f[c]	Orbital Contribution Band gap (eV)
8a	371 299	378	0.9908	H→L (0.699)	333 248	0.8403 0.2337	H→L (0.692) H-1→L (0.545)
8b	406 304 565	373	0.9003	H→L (0.700)	334	0.7496	H→L (0.695)
8c	368 299	391	1.1018	H→L (0.689)	335 263	1.044 0.1072	H→L(0.688) H-1→L (0.624)
8d	425 281 344	374	0.8946	H→L(0.681)	324 249	0.782 0.243	H→L+1(0.562) H-1→L+1(0.459)
8e	535 268	400 370	0.7761 0.2012	H→L (0.622) H→L +1 (0.555)	340 282	0.743 0.110	H→L (0.649) H→L+1(0.484)

[a]Experimental absorption wavelength, [b]Computed absorption wavelength, [c]Oscillator strength

Table 28

Observed UV-visible absorption and computed absorption in gas phase at M06/6-31G(d) for dyes **8a-8e**.

| Dyes | λ_{max}[a] (nm) | TD-DFT | | | | | |
| | | Azo | | | Hydrazone | | |
		Vertical[b] Excitation (nm)	f[c]	Orbital contribution band gap (eV)	Vertical[b] Excitation (nm)	f[c]	Orbital Contribution Band gap (eV)
8a	371 299	404	0.976	H→L (0.708)	368 257	0.746 0.288	H→L (0.706) H-2→L (0.562)
8b	406 304 565	398	0.875	H→L (0.707)	367	0.666	H→L (0.705)
8c	368 299	420	1.087	H→L (0.707)	369 278	0.983 0.125	H→L(0.703) H-2→L (0.547)
8d	425 281 344	396	0.820	H→L (0.665)	351 271	0.721 0.132	H→L+1(0.698) H-2→L+1(0.554)
8e	535 268	442 412	0.515 0.371	H→L (0.560) H-1→L (0.536)	380 333	0.660 0.257	H→L (0.672) H→L+1(0.604)

[a]Experimental absorption wavelength, [b]Computed absorption wavelength, [c]Oscillator strength

Table 29

Observed UV-visible absorption and computed absorption in gas phase at B3LYP/6-311++G(d,p) for dyes **8a-8e**.

Dye	λ_{max}[a] (nm)	TD-DFT					
		Azo			Hydrazone		
		Vertical[b] Excitation (nm)	f[c]	Orbital contribution band gap (eV)	Vertical[b] Excitation (nm)	f[c]	Orbital contribution band gap (eV)
8a	371 299	418	0.986	H→L (0.608)	387	0.740	H→L (0.640)
8b	406 304 565	411	0.890	H→L (0.607)	383	0.671	H→L (0.637)
8c	368 299	442	1.102	H→L (0.613)	392 297	1.005 0.109	H→L(0.643) H-1→L (0.610)
8d	425 281 344	456 389	0.143 0.868	H→L (0.0.587) H→L +1(0.563)	368	0.735	H→L+1(0.639)
8e	535 268	455 396	0.840 0.102	H→L (0.599) H→L+1 (0.636)	405 371	0.562 0.312	H→L (0.596) H→L+1(0.599)

[a] Experimental absorption wavelength, [b] Computed absorption wavelength, [c] Oscillator strength

Table 30

Observed UV-visible absorption and computed absorption in gas phase at CAM- B3LYP/6-311++G(d,p) for dyes **8a-8e**.

Dye	λ_{max}[a] (nm)	TD-DFT					
		Azo			Hydrazone		
		Vertical [b] Excitation (nm)	f[c]	Orbital contribution band gap (eV)	Vertical [b] Excitation (nm)	f[c]	Orbital contribution band gap (eV)
8a	371 299	384	0.9840	H→L (0.698)	340 252	0.8349 0.2178	H→L (0.690) H-1→L (0.524)
8b	406 304 565	380	0.8893	H→L (0.699)	338	0.7453	H→L (0.693)
8c	368 299	399	1.1071	H→L (0.685)	342 254	1.0554 0.1624	H→L(0.683) H-1→L (0.486)
8d	425 281 344	381	0.9194	H→L(0.689)	329 253	0.6135 0.237	H→L+1(0.657) H-1→L+1(0.576)
8e	535 268	403 369	0.8955 0.1116	H→L (0.647) H-1→L (0.571)	344 311	0.7284 0.2701	H→L (0.628) H→L+1(0.244)

[a]Experimental absorption wavelength, [b] Computed absorption wavelength, [c]Oscillator strength

40

Table 31

Observed UV-visible absorption and computed absorption in gas phase at M06/6-311++G(d,p) for dyes **8a-8e**.

Dye	λ_{max} [a] (nm)	TD-DFT					
		Azo			Hydrazone		
		Vertical [b] Excitation (nm)	f [c]	Orbital contribution band gap (eV)	Vertical [b] Excitation (nm)	f [c]	Orbital contribution band gap (eV)
8a	371 299	412	0.868	H→L (0.670)	376	0.742	H→L (0.705) H-2→L (0.562)
8b	406 304 565	405	0.862	H→L (0.707)	372	0.666	H→L (0.705) H-3→L (0.517)
8c	368 299	430	1.038	H→L (0.693)	377 282	0.985 0.119	H→L (0.701) H-2→L (0.543)
8d	425 281 344	401	0.682	H→L (0.615)	357	0.725	H→L+1(0.701)
8e	535 268	442 412	0.708 0.212	H→L (0.625) H-1→L (0.594)	384 346	0.644 0.269	H→L (0.655) H→L+1(0.579)

[a]Experimental absorption wavelength, [b]Computed absorption wavelength, [c]Oscillator strength

List of Figures:

Figure 1. Structures of Synthesized dyes **8a-8e.**

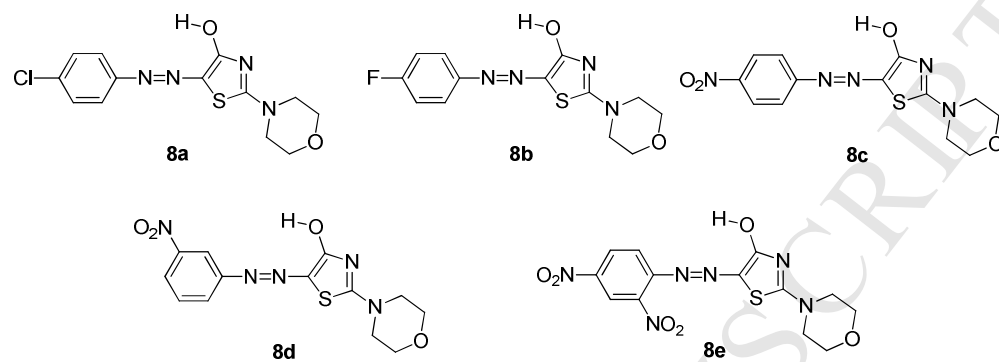**Figure 2**. Dihedral angular twist in azo form of dye **8e**.

B3LYP/6-31G(d)

B3LYP/6-311++G(d,p)
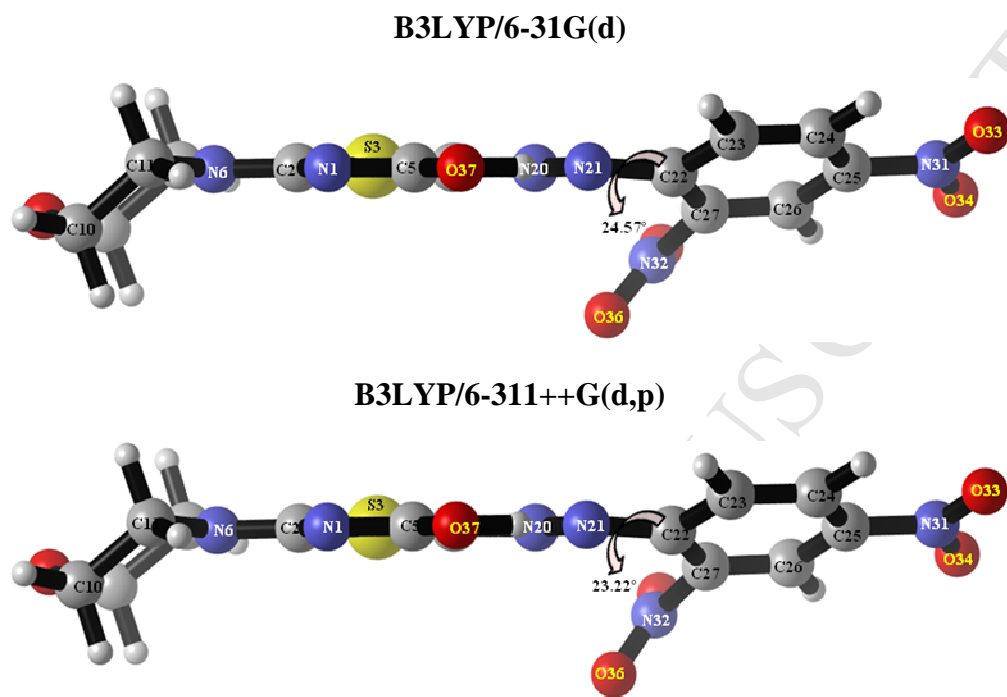
Figure 3. Dihedral angular twist in hydrazone form of dye **8e**.

B3LYP/6-31G(d)

B3LYP/6-311++G(d,p)

Figure 4: Thermogravimetric analysis overlay graph of dyes **8a-8e**.

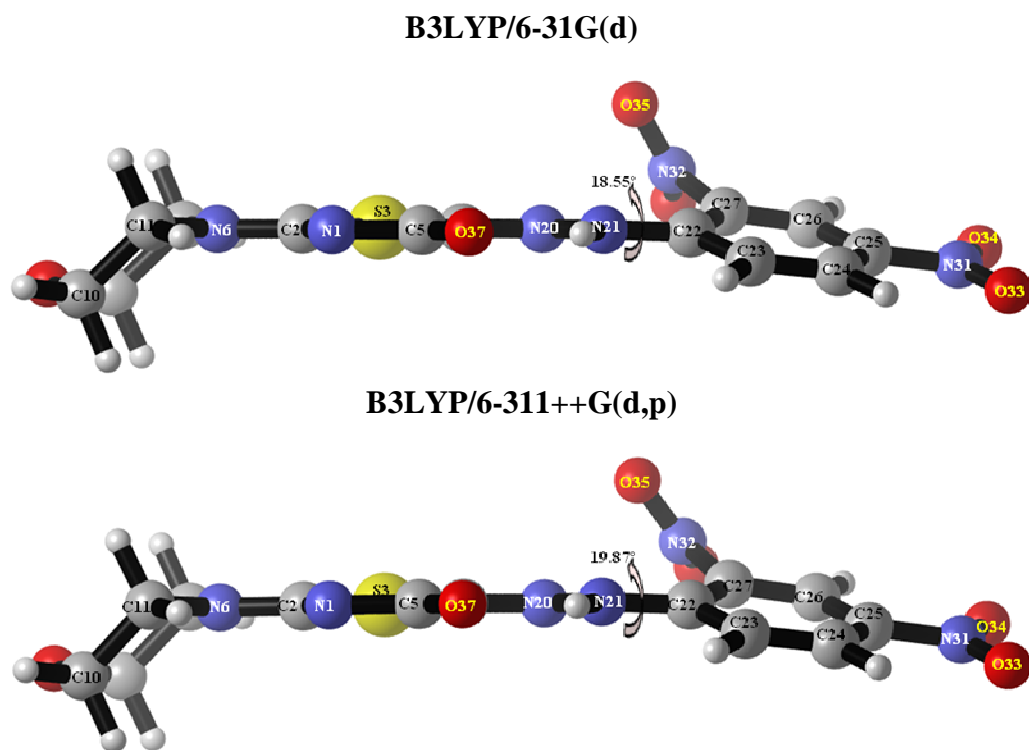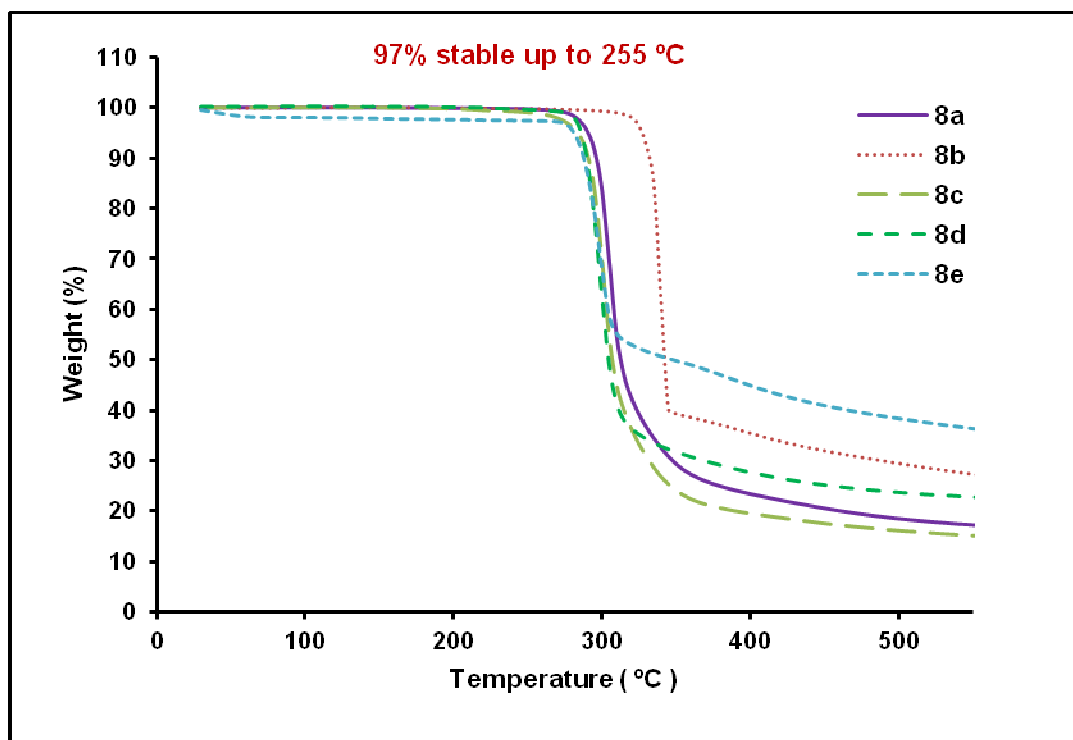**Scheme 1.** Synthesis of 2-morpholin-4-yl-1,3-thiazol-4(5*H*)-one 5 based azo dyes.
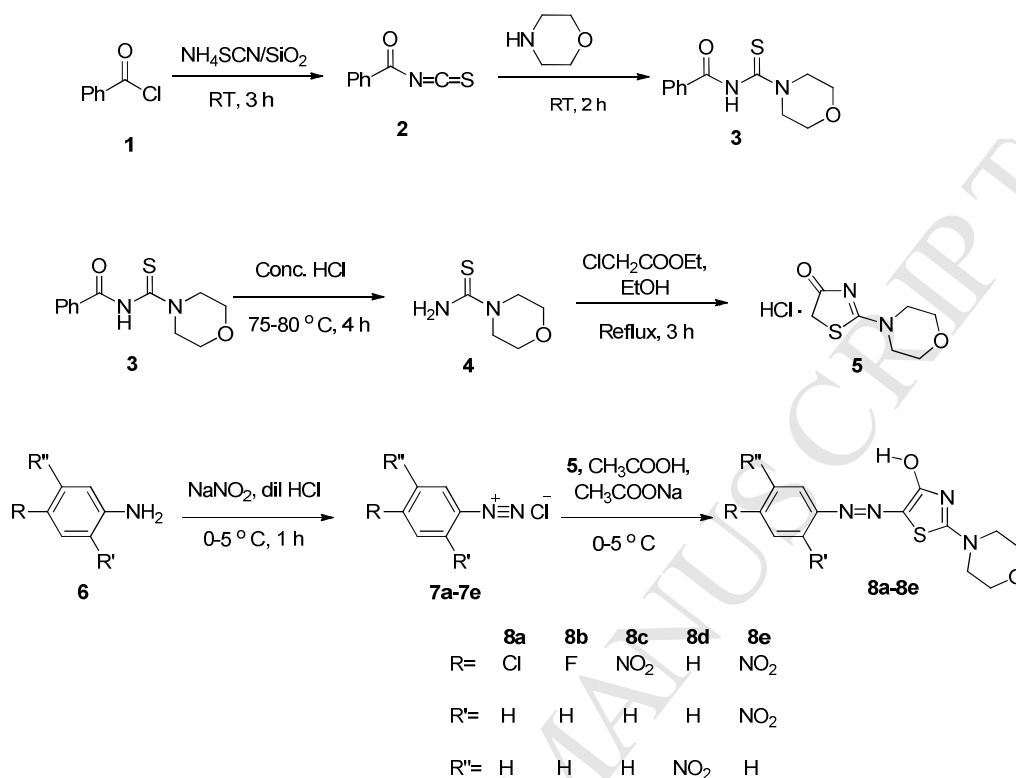

	8a	8b	8c	8d	8e
R=	Cl	F	NO$_2$	H	NO$_2$
R'=	H	H	H	H	NO$_2$
R''=	H	H	H	NO$_2$	H

Highlights

➢ Synthesized azo dyes from 2-Morpholin-4-yl-1,3-thiazol-4(5*H*)-one by simple route

➢ Azo-hydrazone tautomerization has been discussed experimentally and theoretically.

➢ Experimental photophysical properties were supported by computation

➢ Thermal properties were evaluated and compounds are thermally stable